Environmental Science & Technology

pubs.acs.org/est

Article

DDT, Chlordane, and Hexachlorobenzene in the Air of the Pearl River Delta Revisited: A Tale of Source, History, and Monsoon

Lele Tian, Jing Li, Shizhen Zhao,* Jiao Tang, Jun Li, Hai Guo, Xin Liu, Guangcai Zhong, Yue Xu, Tian Lin, Xiaopu Lyv, Duohong Chen, Kechang Li, Jin Shen, and Gan Zhang*

Cite This: *Environ. Sci. Technol.* 2021, 55, 9740−9749

Read Online

ACCESS | Metrics & More | Article Recommendations | Supporting Information

ABSTRACT: Although organochlorine pesticides (OCPs) have been banned for more than three decades, their concentrations have only decreased gradually. This may be largely attributable to their environmental persistence, illegal application, and exemption usage. This study assessed the historic and current regional context for dichlorodiphenyltrichloroethane (DDT), chlordane, and hexachlorobenzene (HCB), which were added to the Stockholm Convention in 2001. An air sampling campaign was carried out in 2018 in nine cities of the Pearl River Delta (PRD), where the historical OCP application was the most intensive in China. Different seasonalities were observed: DDT exhibited higher concentrations in summer than in winter; chlordane showed less seasonal variation, whereas HCB was higher in winter. The unique coupling of summer monsoon with DDT-infused paint usage, winter monsoon with HCB-combustion emission, and local chlordane emission jointly presents a dynamic picture of these OCPs in the PRD air. We used the BETR Global model to back-calculate annual local emissions, which accounted for insignificant contributions to the nationally documented production (<1‰). Local emissions were the main sources of *p,p′*-DDT and chlordane, while ocean sources were limited (<4%). This study shows that geographic−anthropogenic factors, including source, history, and air circulation pattern, combine to affect the regional fate of OCP compounds.

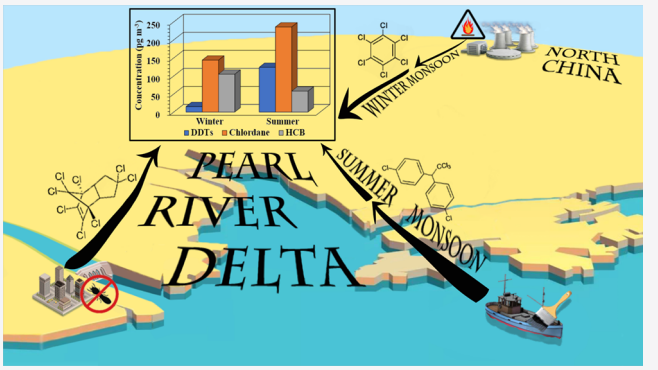

KEYWORDS: *organochlorine pesticides, Pearl River Delta, back-calculated emission, multimedia fate model*

INTRODUCTION

Organochlorine pesticides (OCPs) were first listed in the "dirty dozen" of persistent organic pollutants (POPs) by the Stockholm Convention in 2001,[1] as they are persistent, capable of undergoing long-range atmospheric transport (LRAT), and could bioaccumulate in the food chain; as such, they are a threat to the ambient environment and human health.[2] Although it has been more than three decades since the international ban on OCPs, their concentrations are not declining as rapidly as expected;[3] they are still widely detected around the world,[4−8] even in remote regions, such as in the air and soil of the Tibetan Plateau,[9,10] the deep sea,[11] and the local population[12] of the Arctic. This lack of a rapid decline in OCPs is caused by their inherent persistence,[13] unintentional emission,[14] illegal application,[15] and exemption usage on public health.[16−18]

China is the world's second-largest pesticide producer.[3] OCPs accounted for approximately 80% of national pesticide production during the 1950s−1970s.[2] Dichlorodiphenyltrichloroethane (DDT), chlordane, and hexachlorobenzene (HCB) were selected as model compounds, because they have distinct physicochemical properties and high detection frequencies in the environment. DDT was widely used in cotton fields in China from the 1950s and was banned in 1983, with a historical production of 0.4 million tons, accounting for 20% of global production.[3] After its ban, it was still used in antifouling paint until 2009 for fishing ships[15] and for dicofol production until 2019.[19] As China experiences the most severe termite damage, chlordane was mainly used for termite prevention and control. It was produced in large quantities from 1970 and was banned for all purposes in 2009.[20] In China, although HCB has never been directly used as a pesticide, it is used as an intermediate to produce chlorothalonil,[13] pentachlorophenol (PCP), and pentachlorophenol-Na (PCP-Na).[2] It is also an unintentional byproduct of industrial manufacturing and combustion processes.[14,21]

Received: February 13, 2021
Revised: June 3, 2021
Accepted: June 4, 2021
Published: July 2, 2021

https://doi.org/10.1021/acs.est.1c01045
Environ. Sci. Technol. 2021, 55, 9740−9749

Located in the subtropical region of southern China, the Pearl River Delta (PRD) is one of the most developed regions in the country, with the most extensive pesticide application in history.[3] As such, the PRD is often regarded as a significant source of OCPs in the global context.[22] During the 2000s, we have conducted several monitoring and surveillance campaigns on OCPs in the air of the PRD, using active[22] and passive[23] air sampling techniques. A revisit would provide great benefit in assessing the current regional situation of DDT, chlordane, and HCB, which were first listed by the Stockholm Convention in 2001. This revisit is also under the framework of the National Key R&D Program of China-Towards an Air Toxic Management SYstem in China (ATMSYC).

Ambient air was selected as the sampling medium, because it makes carrying out field experiments easy, is well-mixed to represent regional pollution, and enables high spatiotemporal resolution. Therefore, we aimed to (i) determine the occurrence, spatial distribution, and seasonal variation of selected OCP compounds (DDT, chlordane, and HCB) in the PRD, which represents a typical region with high-speed urbanization in China; (ii) gain new insights into the current status of regional sources and input pathways under a geographic−anthropogenic scene; and (iii) evaluate the effectiveness of the Stockholm Convention implementation and shed light on the sound management of banned OCPs in future. To the best of our knowledge, this is the first time that measurement and modeling have been combined to assess the source and fate of OCPs under a regional geographic−anthropogenic scene.

MATERIALS AND METHODS

Sampling Campaign in the PRD Region. The PRD is one of the most developed Chinese city clusters, located on the southern coast of China. It covers 0.4% of the national land area but contains 8% of the country's population.[24,25] The PRD has experienced the most rapid urban expansion in human history, being a predominantly agricultural region transformed into the world's largest city cluster. As a result, air quality has become a great concern in the PRD over the past decades, because of the rapidly increasing chemical consumption associated with industrialization and urbanization. The PRD is located in a subtropical zone under the strong influence of the Asian monsoon.[22] Due to its unique climate and weather, this region is characterized by complex atmospheric circulation, which plays an important role in the transport and redistribution of air pollutants. For instance, the convergence of cold air from the north and warm air from the south facilitates the accumulation of air pollutants in the PRD.[26]

We selected nine prefecture-level cities of the PRD, Shenzhen, Foshan, Dongguan, Zhongshan, Jiangmen, Zhuhai, Zhaoqing, Huizhou, and Guangzhou, as detailed in Table S1 and Figure S1. All utilized sampling sites are official monitoring stations that are representative of city-level air pollution characteristics. At each site, a high-volume active air sampler (Mingya Instruments Co., Guangzhou, China) was fitted with polyurethane foam plugs (PUFs, 14 cm in diameter × 7.5 cm in thickness, 0.02 g/cm^3 in density) and a quartz fiber filter (QFF, Whatman, 203 mm × 254 mm) to capture pollutants in gaseous and $PM_{2.5}$ phases. Air samples were collected continuously at 24 h intervals for 1 week in winter (January to February 2018) and summer (July to August 2018). The total number of paired samples was 126. Before sampling, the QFFs were baked at 450 °C overnight, and the PUFs were precleaned separately with acetone and dichloromethane (DCM). All samples were delivered to the laboratory and stored at −20 °C before analysis.

Sample Pretreatment and Analysis. The details for sample treatment and instrumental analysis are provided in previous studies.[6,14] In short, QFFs and PUFs were spiked with ^{13}C-labeled *trans*-chlordane as the recovery surrogate and extracted in a Soxhlet apparatus for 24 h with DCM. The extracts were concentrated via rotary evaporation and solvent-exchanged into hexane at a reduced volume of 0.5−1 mL. They were then purified using a multilayer acidified silica gel column and concentrated in a vial under gentle nitrogen. $^{13}C_{12}$-labeled PCB 141 was added as an internal standard before instrumental analysis. Samples were analyzed on an Agilent 7890A/7000A GC−MS/MS with a CP-Sil 8 CB column (50 m × 0.25 mm × 0.12 μm) in a multiple reaction monitoring (MRM) mode. The precursor/product ions and retention times are listed in Table S2.

Quality Assurance and Quality Control (QA/QC). QA/QC was conducted using field blanks, procedural blanks, and surrogate spiked recoveries. Most congeners were not detected in the field blanks or procedural blanks. The average recovery rate of $^{13}C_{12}$-labeled *trans*-chlordane was 108 ± 22%. The inlet degradation of DDT was checked by injecting a *p,p′*-DDT standard for every 10 samples and controlled within 15%. The reported concentrations were corrected for the blanks and surrogate recoveries. The method detection limits (MDLs) were calculated as the average of field blanks plus triple standard deviations. MDLs were assigned as three times instrumental detection limits (IDLs) if a congener was not detected in the field blanks or procedural blanks. IDLs were defined as the amount of analytes generating a signal-to-noise ratio of 3:1 using the lowest standard level, assuming an increasing linear response. The IDLs and MDLs of selected OCPs ranged from 11−71 pg and 0.005−1.11 pg/m^3 as detailed in Table S3. The breakthrough was assessed and corrected for HCB as detailed in Text S1.

Backward Trajectory Simulation and Potential Source Contribution Function (PSCF) Model. Backward particle release simulation, considering the dispersion processes in the atmosphere, has been widely used to identify the history of air masses.[27] In this study, it was performed using the Hybrid Single-particle Lagrangian Integrated Trajectory model (HYSPLIT 4.0, https://ready.arl.noaa.gov/HYSPLIT.php).[27,28] The input meteorological data were obtained from the Gridded Meteorological Data Archives of the Air Resources Laboratory (https://ready.arl.noaa.gov/archives.php). All trajectories were calculated at 1 h intervals, and the cluster analysis of 72 h backward trajectories is presented in Figure S2.

The PSCF model can be described as a conditional possibility, characterized by using trajectories to the sampling sites to determine the spatial distribution of possible geophysical source locations.[29,30] Due to the limited sample size in this study, the PSCF outputs could only represent potential source directions rather than locations. This is because this approach evenly distributes weight along the path of the trajectories.[31] The *ij*th component of a PSCF field ($PSCF_{ij}$) is defined as:

$$PSCF_{ij} = \frac{m_{ij}}{n_{ij}}$$

https://doi.org/10.1021/acs.est.1c01045
Environ. Sci. Technol. 2021, 55, 9740−9749

Table 1. Summary of DDTs, Chlordane, and HCB in the Air of Nine Cities in the PRD Region (n = 126), Based on the Summed Concentrations in the Gaseous and $PM_{2.5}$ Phases[a]

season	winter			summer		
pg/m^3	min	max	mean ± std	min	max	mean ± std
HCB	55	223	105 ± 35	2	132	58 ± 27
cis-chlordane	1	267	44 ± 65	1	361	71 ± 66
trans-chlordane	5	641	99 ± 143	5	1070	165 ± 169
chlordane	7	893	144 ± 208	6	1431	236 ± 233
TC/CC	1.7	6.4	2.4 ± 0.6	1.6	4.5	2.3 ± 0.4
o,p'-DDT	<MDL[b]	29	3 ± 7	<MDL	89	30 ± 21
p,p'-DDT	1	87	10 ± 18	9	389	80 ± 74
o,p'-DDD	<MDL	1	0.2 ± 0.2	<MDL	6	2 ± 1
p,p'-DDD	<MDL	2	0.5 ± 0.5	<MDL	10	3 ± 3
o,p'-DDE	<MDL	2	0.2 ± 0.3	<MDL	5	1 ± 1
p,p'-DDE	<MDL	7	1 ± 2	<MDL	29	7 ± 6
DDTs	2	123	15 ± 27	11	516	124 ± 104
p,p'-DDT/DDTs	0.26	0.87	0.60 ± 0.14	0.33	0.92	0.63 ± 0.09
DDT/DDTs	0.50	0.95	0.80 ± 0.10	0.72	0.97	0.88 ± 0.04
p,p'/*o,p'*-DDT	0.87	38.7	5.1 ± 5.7	0.84	19.7	3.0 ± 2.5
p,p'-DDT/*p,p'*-DDE	1.0	43.4	9.4 ± 8.1	2.5	94.9	14.1 ± 16.3

[a]HCB concentration has been corrected for the breakthrough level as presented in Text S1 and Table S8. [b]MDL is the method detection limit and its specific value is listed in Table S3.

where n_{ij} represents the number of trajectory endpoints falling in the ijth cell; and m_{ij} is the number of air masses from the same cell loaded with species whose concentrations are greater than the set criterion values. The threshold values were set as the 75th percentile of the OCP concentration to identify potential source directions. An arbitrary weight function was used to better reflect the uncertainty caused by the limited endpoints.[32]

Observation-Based Emission Estimate. We employed a "top-down" approach to retrospectively quantify the emissions of target OCP compounds by combining field measurements and modeling, which has been widely used to predict the industrial chemicals in urban areas worldwide.[33,34] It overcomes the disadvantage of poor or incomplete emission data required by the "bottom-up" approach, by utilizing chemical production, usage, and disposal data together with emission factors.[33] A level IV global-scale multimedia contaminant fate model, the Berkeley-Trent (BETR) Global model (http://betrs.sourceforge.net/), was selected to back-calculate emissions, which has been fully evaluated and extensively used to understand the global dynamics of persistent semivolatile pollutants.[35−37] The simulation was performed in Python (https://www.python.org/), at a spatial resolution of 3.75°. Although the spatial resolution is relatively low, it could help to generalize and "even out" the uncertainty, which has been demonstrated to work well for regional studies.[35]

Each grid cell contains seven compartments: upper atmosphere, lower atmosphere, vegetation, freshwater, ocean, soil, and freshwater sediment.[36] The target region for the emission estimate in the model was Grid-T1, as shown in Figure S3. Although one site (Zhuhai) was outside the grid, this does not affect the simulation as the emission rate was assumed to be proportional to land area. The main input parameters, including physicochemical properties and environmental half-lives, were predefined in the BETR Global model, as shown in Table S4. The propagation of uncertainty from physicochemical parameters in the emission estimates was evaluated by a first-order analytical uncertainty analysis, assuming a linear relationship between inputs and outputs.[38] A confidence factor (Cf) was assumed for each physicochemical parameter as presented in Table S4.[38]

Local Emission Estimate. The emission rate into air was adjusted such that the median-modeled concentrations in the lower air of the target grid were equal to the median measurements as suggested.[33] The local emissions could be quantified by the incremental chemical concentration of the target region compared to background sites that were located upwind of the region. Due to variance in the origin of air masses at different sampling sites during summer (Figure S2), there were no available upwind background sites that could be utilized. As such, the simulation was only restricted to winter, and the northeastern-most site (Huizhou) was selected as the upwind background site to represent the external OCP input in winter. The minimum and median OCP concentrations in Huizhou were used to represent the worst-case and moderate local emission scenarios, respectively. The contribution fraction of local emission (f_{local}) was derived from the difference in regional OCP concentration (C_{PRD}; median value of the PRD sites) and external input concentration (C_{ex}) divided by the regional level ($f_{local} = (C_{PRD} - C_{ex})/C_{PRD}$).

Ocean Source Estimate. The coastal areas of southern and eastern China (see Figure S3, Grid-S1 to S4) were simulated as ocean source regions that may influence OCP levels in the PRD. OCP concentrations in seawater and ocean air were selected from the literature and used as inputs for source grids (Table S5). The annual inventory of OCPs in seawater was derived by multiplying the concentrations (annual mean) by the volume of the seawater compartment in ocean grids. This annual inventory was converted into the emission rate (mol/h) and was provided as an input to the ocean grids. The PRD grid was set as the receptor lacking in initial OCP inputs. The simulation was conducted for 3 years, which was a sufficient duration to reach a stable state, where the results of the third year were used. The ocean source contributions were calculated using the OCP concentrations in the PRD grid (Grid-T1) divided by the measured concentrations in the PRD (median value).

https://doi.org/10.1021/acs.est.1c01045
Environ. Sci. Technol. 2021, 55, 9740−9749

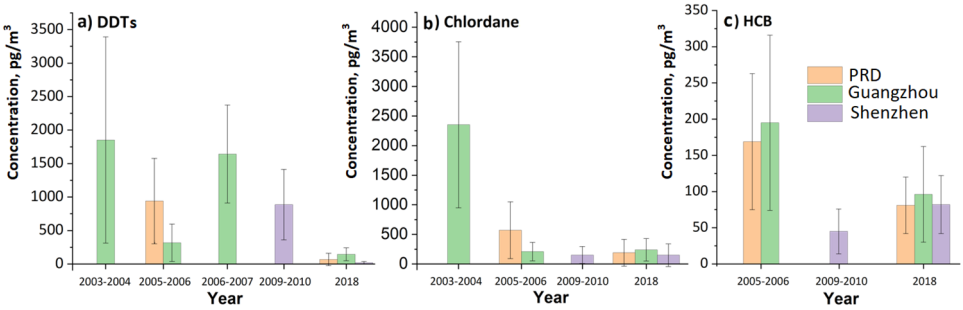

Figure 1. OCP trends (mean ± standard deviation) over the 2003−2018 period in the PRD region based on this study and the literature.[22,23,39−41] The specific values are presented in Table S9.

RESULTS AND DISCUSSION

This section describes the general characteristic of OCPs in the air of the PRD region and then examines the spatial and seasonal configuration of OCP sources and potential air transport. This will be followed by a quantitative estimation of current local emission, and an assessment of contributions from the ocean using a multimedia fate model.

Profile of OCPs in the PRD. This study determined nine target compounds, including DDTs (sum of *o,p′*-DDT, p,p′-DDT, *o,p′*-DDD, *p,p′*-DDD, *o,p′*-DDE, and *p,p′*-DDE), chlordane (*trans*-chlordane (TC) and *cis*-chlordane (CC)), and HCB. Their average concentrations and diagnostic ratios are summarized in Table 1, and their spatial distributions are shown in Figure S4. Detailed OCP concentrations in the gaseous and $PM_{2.5}$ phases are presented in Tables S6−S8. A comparison with the literature is presented in Figure 1 and detailed in Table S9. All measured compounds were predominant in the gaseous phase, accounting for up to 95% of the total concentration in the atmosphere. Detection rates were relatively low ranging from 5 to 75% in the $PM_{2.5}$ samples yet reaching 69−100% in the gaseous samples. HCB and chlordane were detected in all gaseous samples. Therefore, only the summed concentrations in gaseous and $PM_{2.5}$ phases are further discussed. In general, the average airborne OCP levels were ranked in descending order as follows: chlordane > HCB > DDTs in winter and chlordane > DDTs> HCB in summer.

DDT. A wide range of DDT concentrations were observed (2−516 pg/m^3) with significant seasonality (Kruskal−Wallis H test, $p < 0.001$). The average DDT concentration in winter was 15 ± 27 pg/m^3, which was one order of magnitude lower than that in summer (124 ± 104 pg/m^3). *p,p′*-DDT was the dominant isomer in 87% of the samples, contributing an average of 62 ± 12% with a level of 45 ± 64 pg/m^3. Significant correlations were found between DDT and its metabolites (all $R^2 > 0.90$, $p < 0.001$), possibly implying similar sources.

As summarized in Figure 1a and Table S9, DDT decreased the most among the three types of OCPs, with a maximum 30-fold reduction from ∼2000 pg/m^3 to ∼70 pg/m^3 since the 2000s.[23,41] All DDT isomers were observed to decline by an order of magnitude in the PRD, compared to the reported level in 2003−2004.[22] The current DDT level (69 ± 93 pg /m^3) in the PRD was relatively low, which is an order of magnitude lower than that in northern China (206 ± 405 pg/m^3)[42] and other surrounding countries, including Nepal (220 ± 359 pg/m^3),[9] Pakistan (350 ± 240 pg m^3),[43] and Vietnam (516 ± 401 pg /m^3 in summer and 1555 ± 1068 pg/m^3 in winter).[44]

The ratios of various DDT isomers offer an insight into their source information. First, the ratios of (*o,p′*-DDT + *p,p′*-DDT)/DDTs could be used to assess the long-term weathering and DDT biotransformation, as *p,p′*-DDT principally degrades to *p,p′*-DDD and/or *p,p′*-DDE by microorganisms under anaerobic or aerobic conditions.[45] The ratios of (*o,p′*-DDT + *p,p′*-DDT)/DDTs > 0.5 or < 0.5, may indicate the relatively "fresh" inputs or the predominance of aged (microbially degraded) DDTs derived from historical residues, though the boundary between "old" or "new" sources is not very clearly identified.[46] These results suggest that the fresh DDT emission may still exist, given the observed high *p,p′*-DDT concentrations and its percentage (62 ± 12%) among the DDTs. The ratios of *o,p′*-DDT/*p,p′*-DDT were between 0.20 and 0.26 in technical DDT, while the "dicofol-type DDT" was characterized by a higher *o,p′*-DDT/*p,p′*-DDT concentration ratio (∼7).[19,42] Therefore, the ratio of *o,p′*-DDT/*p,p′*-DDT can be used to distinguish technical DDT or dicofol in the environment. In this study, the ratio of *o,p′*-DDT/*p,p′*-DDT was 0.40 ± 0.24 indicating that technical DDT was the dominant contributor and thus of greater importance than the dicofol-type DDT.

We also utilized the isomeric ratios of DDT to identify possible source contributions, following previous studies.[46,47] This approach assumed the worst scenario in which DDT in the environment only comes from dicofol formulation and technical DDT. Because of the dominant *p,p′*-DDT contribution to DDTs (>80%), fresh DDT should be the main source. Thus, it is reasonable to ignore the legacy DDT here. Based on the rough estimation, if assuming only dicofol-type DDT and technical DDT exist, the dicofol-type DDT may contribute up to ∼10% of the total sources. This is considerably lower than the ∼50% in the PRD during 2003−2004 reported in a previous study.[47] This indicates strong effectiveness of suspending dicofol production in 2014, owing to its DDT impurities.[19] The current technical DDT may largely be sourced from possible ongoing use of DDT-infused antifouling paints in the coastal regions of China.[23,48,49]

Chlordane. Chlordane (TC + CC) levels ranged between 6 and 1431 pg/m^3 in the PRD, with less significant seasonality compared to DDT (Kruskal−Wallis H Test, $p < 0.001$). The chlordane concentration in summer was 236 ± 233 pg/m^3, which was higher than that in winter (144 ± 209 pg/m^3). Its level fluctuated drastically at the same site by a factor of 10. The highest chlordane concentration occurred during winter in Dongguan (468 ± 339 pg/m^3). TC (5−1070 pg/m^3) dominated the chlordane family accounting for 61−86%, contrary to the previously observed CC domination.[50] A good

https://doi.org/10.1021/acs.est.1c01045
Environ. Sci. Technol. 2021, 55, 9740−9749

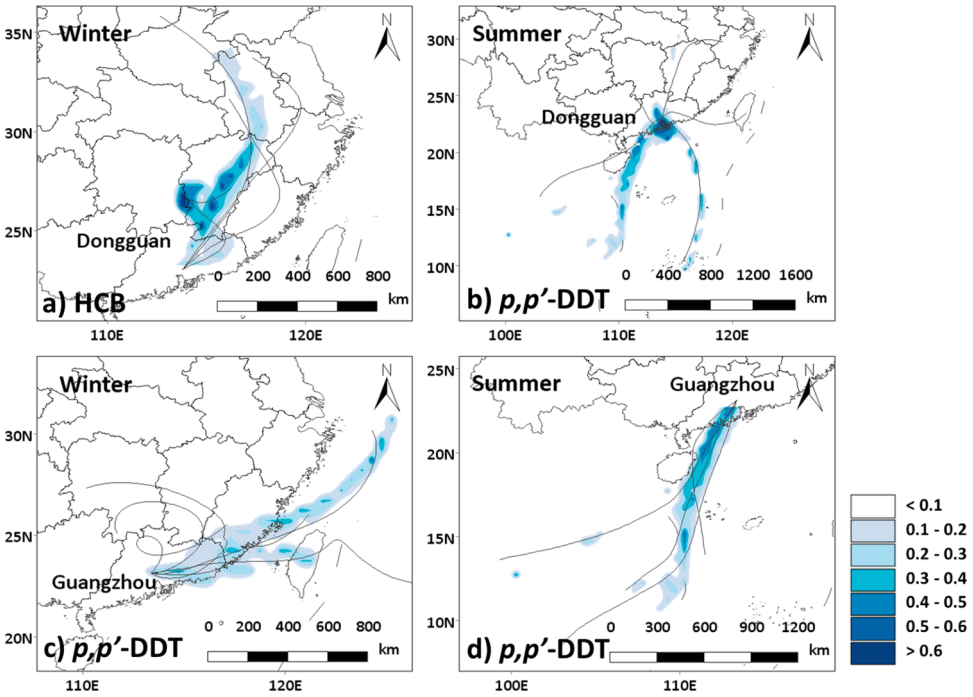

Figure 2. PSCF results of OCP compounds in Dongguan and Guangzhou, which mainly represented the source direction due to limited sample size. The black lines indicate clustered 72 h backward trajectories from the HYSPLIT model (https://www.arl.noaa.gov/hysplit/hysplit/).

correlation between TC and CC was observed, with an R^2 = 0.95 (p < 0.001).

A rapid downtrend was observed for chlordane, at an order of magnitude lower than that measured in the 2000s in the PRD (from ∼2000 pg/m^3 to ∼200 pg/m^3).[22] It is at an intermediate level in the PRD, comparable to that in northern China (295 ± 555 pg/m^3)[42] and other Asian countries.[44] The chlordane production peak occurred around 2003,[20] which is similar to the trend of observed chlordane concentration as in Figure 1b. The declining trend appears to have recently decelerated at a relatively steady level of ∼200 pg/m^3 over the past decade.[39,41] The Chinese government banned chlordane production for all purposes in 2009.[20] This stable trend could have resulted from the gradual release of its historical legacy in building foundations and dams in the PRD, which were mainly constructed during the 1960s−1970s.[53]

The annual average TC/CC ratio in the air of the PRD was 2.4 ± 0.5, characterized by a very stable trend without a seasonal difference (Kruskal−Wallis H Test, p > 0.5). A significant increase was observed in these TC/CC ratios, compared to previous studies (TC/CC: 0.3−1.4).[22] The reported ratio of TC/CC in technical chlordane is 0.76−0.8 in the PRD.[52] When adjusted for vapor pressure difference by multiplying an enhancement factor of 1.39,[53] this ratio of TC/CC becomes 1.1, owing to higher vapor pressure of TC compared to that of CC. This difference in the ratio between the ambient air and technical chlordane may be a result of the differential removal of TC and CC.[54] The heptachlor source could also possibly contribute to TC, as its technical product in North America was found to be contaminated with 18−22% TC but only 2% with CC.[55] Similarly, a high ratio of TC/CC (>1.2 of technical chlordane) was also recently observed in the air of other Chinese regions[56,57] and foreign countries, such as Vietnam.[44]

HCB. The HCB level in the PRD averaged 81 ± 39 pg/m^3 during the sampling period. In contrast to the seasonality of DDT, its concentration in winter (105 ± 35 pg/m^3) was double that in summer (58 ± 27 pg/m^3), with a significant seasonal difference (Kruskal−Wallis H Test, p < 0.001). The highest HCB concentration was 138 ± 38 pg/m^3 during winter in Zhaoqing. The HCB level was more stable with a smaller standard deviation than DDT and chlordane, indicating that it was well-mixed in the atmosphere.

HCB concentration showed a gradually decreasing trend from 2005 in the PRD[23,41] as shown in Figure 1c. This is because HCB has never been used as a pesticide in China and is mainly unintentionally produced from industrial manufacturing and combustion processes, which poses a substantial challenge in terms of its effective control.[14] Our reported value is at a moderate level within China and across the world. It is lower than concentrations in northern China (∼200 pg/m^3)[42] and higher than concentrations in the Nam Co of Tibet (∼20 pg/m^3).[10] Compared to other countries, HCB concentrations in the PRD are much lower than those reported in Vietnam (∼600 pg/m^3),[44] while they are higher than those reported for Pakistan (∼30 pg/m^3)[43] and Spain (∼40 pg/m^3).[58]

Seasonal Coupling of Sources and Input Pathways. *Summer Monsoon and DDT Plume.* During the sampling period, the summer monsoon dominated in summer, while the winter monsoon prevailed in winter, as indicated by the backward trajectories in Figure S2, which was well-matched with DDT seasonality. Specifically, DDT concentrations in summer were much higher than those in winter, potentially due to the summer monsoon carrying the primary and/or secondary emissions of DDT from the coastal region into the PRD. It has been demonstrated that large parts of the tropical and southern midlatitude ocean could have been changed from a net sink into a net emission (volatilization) source since the 1980s.[59] Therefore, DDT could possibly continually re-enter the atmosphere from the ocean, prior to its dissolution in a recurring cycle.[59] This may not be the case in this study, as DDT was found to be highly degraded ((*o,p'*-DDT + *p,p'*-

https://doi.org/10.1021/acs.est.1c01045
Environ. Sci. Technol. 2021, 55, 9740−9749

DDT)/DDTs < 0.5) in the surface seawater of the South and East China Sea.[5,60] Conversely, the detected DDT was much fresher in our air samples ((*o,p′*-DDT + *p,p′*-DDT)/DDTs > 0.7), which could mainly be from primary sources as opposed to secondary sources emitted from the sea.

DDT-infused antifouling paint could be a potential ongoing source of primary emissions. Our summer sampling campaign was conducted within an annual fishing suspension period (from May to August) in the South China Sea region. During this period, fishing ships were mandatorily moored at ports and many were subjected to repainting,[22] allowing a large amount of DDT in the antifouling paint to enter the atmosphere.[15] Sampling sites closer to the sea showed higher DDT levels (e.g., Zhuhai; Figure S4), indicating that DDT was likely sourced from the coastal region. Previous studies have also demonstrated the potential ongoing use of DDT-infused antifouling paints in the coastal regions of China,[48,49] where there is a decreasing trend in *p,p′*-DDT concentrations with an increasing distance from the harbor to the inland.[5,61]

During the summer sampling campaign, air masses mainly originated from the South China Sea and entered the PRD through the Pearl River estuary, as shown in Figures S2 and S6. According to the PSCF results in Figure 2, DDT was mainly sourced from the direction of the sea and was less related to the northern inland region. In winter, DDT levels in Guangzhou were an order of magnitude higher than those in other sampling cities. The air masses arriving at Guangzhou originated from the East China Sea and South China Sea, while other sites mainly received air masses from northern inland regions (Figures S2 and S6). In addition, mesoscale circulations, such as sea-land breezes, also play an important role in the distribution and transport of organic pollutants in coastal cities.[62] Therefore, we confirmed that the inland-ward summer monsoon may introduce DDT from coastal regions into the inland of the PRD. In contrast, the opposite seasonality was observed in Vietnam, where winter had a higher DDT, mainly influenced by air masses from the South China Sea.[44] Therefore, monsoons could be the main carrier of DDTs in the PRD.

Kinetically Limited Release of Chlordane. Historically, technical chlordane was mixed with concrete and "locked" in foundations or dams to prevent termites during construction.[50] We observed a minor change in the chlordane concentration between summer and winter, implying a large contribution of the slow kinetically limited release of "old" chlordane from foundations/dams and a lower contribution of temperature-controlled evaporation from surfaces. The widely varied chlordane concentrations with two orders of magnitude difference also indicated that it was mainly from a scattered local point-source. Chlordane concentrations that are an order of magnitude higher in the PRD than in northern China[42] and other Asian countries[43,44] highlight the historically large amount of chlordane applied in the heavily termite-affected region.[20] During the 1960s−1970s, Guangdong Province, where the PRD is located, built ∼8000 reservoir dams during the 1960s−1970s, accounting for ∼10% of the total documented dams constructed across China.[51] In the 1950s, China had begun production of chlordane on a pilot scale, reaching an industrial scale production peak in the 2000s.[20] This could have resulted in a large amount of chlordane that is locked inside the dams and/or buildings that may undergo a kinetically limited release, via cracks in the old dams and foundations or the occasional perturbation during maintenance.[51]

Winter Monsoon and Combustion-HCB Prevalence. Although HCB has never been used as a pesticide in China, it is an intermediate to produce other industrial products[2] and could be unintentionally produced from industrial manufacturing and combustion processes.[14] As depicted in the PSCF results in Figures 1 and S5, HCB in winter was mainly sourced from the northern direction of the PRD region at all sampling sites (Figure 2) and then transported via the winter monsoon. The low summer/winter ratio in HCB concentrations (0.63 ± 0.37) indicated that the seaward source in summer was less intensive than the terrestrial source in winter. This seasonal characteristic ruled out the dominant sources of intentional emission and/or secondary emission, except for thermal processes and combustion. In northern China, a large number of biofuels and fossil fuels are used for heating in winter, emitting high concentrations of HCB.[14] Although Guangzhou received air masses from different origins, it gained a similar HCB level compared to other cities (Figure S4), indicating that HCB was well-mixed in ambient air and less sensitive to the monsoon compared to DDT. In addition, a lower mixing boundary layer height may increase pollutant concentrations in winter.[63]

Derived Local Emissions. The local OCP emission rates derived from our model calculations in the PRD are summarized in Table 2, in units of per capita and per square meter emissions. The annual OCP emissions in the PRD grid were estimated assuming that emissions were directly proportional to the population or land area in the PRD. Combining the BETR Global model with the measurements, the back-calculated total emissions of HCB, *p,p′*-DDT, and chlordane were approximately 2.2−3.8 t/y in the PRD under the moderate scenario. This estimated emission implies an insignificant contribution to the national documented production (less than 1‰), indicating that remarkable effectiveness was obtained in the PRD under the implementation of the Stockholm Convention. The larger contribution of chlordane to its historical production could be because its ban for all-purpose usage only occurred in 2009.[20]

This study attempts to provide a snapshot of the emission rates of selected OCPs in the PRD under the worst-case scenario by combining atmospheric measurements and the fugacity model. It would be beneficial to confirm the results of this study with "bottom-up" estimates or to compare them with other similar "top-down" modeling studies.[33] However, to the best of our knowledge, relevant modeling work on pesticidal POPs is very rare, and limited studies on their inventory development have been carried out. An inventory of technical chlordane production between 1970 and 2008 across China was developed, lacking congener-specific production estimates.[20] Additionally, a historical inventory of DDT was also calculated without modeling the atmospheric concentrations.[64] These challenges are severer regarding the estimation of HCB emissions largely owing to unintentional emissions, with limited knowledge of sources and emission factors.

Contributions of Local Emissions and Ocean Sources. In this study, the contributions of local emissions and ocean sources to the PRD grid were quantified for selected OCP compounds, as shown in Table 3. CC and TC were recognized as mainly originating from local release (range: 85% (moderate scenario)−93% (worst-case scenario)) in winter, while their

https://doi.org/10.1021/acs.est.1c01045
Environ. Sci. Technol. 2021, 55, 9740−9749

Table 2. Atmospheric Emission Rates of Selected OCP Compounds in the PRD

	emission in winter (moderate scenario)				emission in winter (worst-case scenario)				
compound	kg/d	t/y	μg/(capita d)[a]	ng/(m² d)[b]	kg/d	t/y	μg/(capita d)	ng/(m² d)	‰[c]
HCB	0.52(0.50−0.54)	0.19(0.18−0.20)	0.87(0.84−0.89)	9.4(9.1−9.7)	2.9(2.8−3.0)	1.1(1.0−1.1)	4.8(4.7−5.0)	52(50−54)	0.002−0.14
p,p′-DDT	0.29(0.24−0.36)	0.11(0.09−0.13)	0.48(0.39−0.59)	5.2(4.3−6.4)	0.34(0.28−0.42)	0.12(0.10−0.15)	0.56(0.46−0.69)	6.1(5.0−7.5)	<0.001
CC	2.1(1.5−2.8)	0.76(0.56−1.0)	3.5(2.5−4.7)	37(27−51)	2.3(1.7−3.1)	0.83(0.61−1.1)	3.8(2.8−5.1)	41(30−56)	0.31−0.60
TC	5.0(3.7−6.8)	1.8(1.3−2.5)	8.3(6.1−11)	90(66−120)	5.3(3.9−7.2)	1.9(1.4−2.6)	8.8(6.5−12)	95(70−130)	
sum	7.9(5.9−10)	2.9(2.2−3.8)	13(9.9−17)	142(110−190)	11(8.6−14)	3.9(3.1−5.0)	18(14−23)	195(160−250)	0.004−0.009

[a]Based on a population of ca.6.0 × 10⁸ inhabitants in nine cities of the PRD in 2018. [b]Based on a land area of 5.5 × 10¹⁰ m² in the PRD in 2018. [c]The percentage of annual emission to the total national documented production was calculated. The historical production was selected from the literature for HCB,[13] *p,p′*-DDT, and chlordane.[65]

Table 3. Contribution of Local Emission (in Winter) and the Ocean Source (in Summer and Winter) for Selected OCPs in the PRD

	local emission contribution (%)		ocean source contribution (%)	
compound	moderate scenario	worst-case scenario	summer	winter
HCB	6.0	33	36	40
p,p′-DDT	60	70	0.26	2.6
CC	85	93	0.68	3.9
TC	85	89	1.8	1.4

ocean sources were insignificant in summer and winter (<4%). This estimation also supports our speculation that chlordane mainly originates from the slow kinetically limited release of "old" chlordane sealed in foundations/dams, with limited contributions from secondary evaporation off surfaces. Similarly, *p,p′*-DDT was mainly contributed by local emissions ranging from 60 to 70%, with a negligible portion from the ocean source (<3%), which is consistent with the inference that DDT-infused paint is most likely the main contributor instead of the re-evaporation from the ocean surface. The estimated local contributions of HCB ranged from 6.0% (moderate scenario) to 33% (worst-case scenario) in winter, indicating that external sources are the main contributors of HCB. However, ocean sources contributed similar levels over winter and summer.

Limitations and Implications. Although previous studies have demonstrated that the back-calculation approach is useful,[33,34] it comes with several limitations. First, the estimated results highly relied on the quality and quantity of atmospheric measurements used to retrospectively model OCP concentrations in ambient air. Our observation sites are all located in urban areas, which may have led to overestimated emissions. Second, the initial concentrations in soil, water, and sediment were not considered in the simulation, and these compartments may also play roles as secondary sources. Therefore, the actual emissions are expected to be lower than our estimates. Notably, the back-calculated emissions were only valid for the periods and locations of the field measurements, and the spatial variability within the modeled region was not captured. The sensitivity of background concentrations in air and the physicochemical parameters were calculated in this study. However, the uncertainty of other input parameters (e.g., meteorological data) was not evaluated because of the high computational cost required for the applied global model.

The sampling campaign was only implemented for 1 week in winter and summer because of limited time and high labor costs. However, this limitation does not outweigh the merits. A snapshot of pesticidal POPs in the PRD region is integrated and presented in terms of a geographic−anthropogenic scene. Our results clearly reflect the combined configuration of different sources, transport, and fate of chemicals, leading to varied pollution characteristics, taking HCB, DDTs, and chlordane as elegant examples. The unique coupling of the summer monsoon with DDT-infused paint usage, the winter monsoon with HCB-combustion emission, as well as the historical "sealed" chlordane jointly presents a dynamic picture of these OCP compounds in the air of the PRD. This study proposed a geographic−anthropogenic scenario, including source, history, and air circulation patterns, which could be

https://doi.org/10.1021/acs.est.1c01045
Environ. Sci. Technol. 2021, 55, 9740−9749

used exclusively to fully understand the fate of OCP compounds in a region.

Although effective reduction has taken place, illegal technical DDT in antifouling paints for ships continues to be a problem. Dicofol-type DDT is very likely to be diminished, particularly after the enlistment of dicofol by the Stockholm Convention in 2019. The release of chlordane in urban construction foundations and hydraulic dams is very slow due to kinetic control, accompanied by secondary emissions from various surfaces. HCB and other byproducts, such as unintentionally produced POPs from thermal processes, will not fade out. These findings highlight the potentially ongoing sources of POPs, even after decades of regulations aimed at reducing or eliminating such sources. Industries and communities should better manage thermal processes and combustion to gradually address these ongoing issues. Long-term continuous sampling campaigns will be of great help in assessing the effectiveness of the Stockholm Convention implementation.

■ ASSOCIATED CONTENT

Supporting Information

The Supporting Information is available free of charge at https://pubs.acs.org/doi/10.1021/acs.est.1c01045.

The collection efficiency estimation, sampling information, instrumental method, detection limits, detailed OCP data set and comparison with the literature, backward trajectories, and PSCF results (PDF)

■ AUTHOR INFORMATION

Corresponding Authors

Shizhen Zhao − *State Key Laboratory of Organic Geochemistry and Guangdong-Hong Kong-Macao Joint Laboratory for Environmental Pollution and Control, Guangzhou Institute of Geochemistry, Chinese Academy of Sciences, Guangzhou 510640, China; CAS Center for Excellence in Deep Earth Science, Guangzhou 510640, China;* orcid.org/0000-0003-1534-9283; Email: zhaoshizhen@gig.ac.cn

Gan Zhang − *State Key Laboratory of Organic Geochemistry and Guangdong-Hong Kong-Macao Joint Laboratory for Environmental Pollution and Control, Guangzhou Institute of Geochemistry, Chinese Academy of Sciences, Guangzhou 510640, China; CAS Center for Excellence in Deep Earth Science, Guangzhou 510640, China;* orcid.org/0000-0002-9010-8140; Email: zhanggan@gig.ac.cn

Authors

Lele Tian − *State Key Laboratory of Organic Geochemistry and Guangdong-Hong Kong-Macao Joint Laboratory for Environmental Pollution and Control, Guangzhou Institute of Geochemistry, Chinese Academy of Sciences, Guangzhou 510640, China; University of Chinese Academy of Sciences, Beijing 100049, China*

Jing Li − *State Key Laboratory of Organic Geochemistry and Guangdong-Hong Kong-Macao Joint Laboratory for Environmental Pollution and Control, Guangzhou Institute of Geochemistry, Chinese Academy of Sciences, Guangzhou 510640, China*

Jiao Tang − *State Key Laboratory of Organic Geochemistry and Guangdong-Hong Kong-Macao Joint Laboratory for Environmental Pollution and Control, Guangzhou Institute of Geochemistry, Chinese Academy of Sciences, Guangzhou 510640, China*

Jun Li − *State Key Laboratory of Organic Geochemistry and Guangdong-Hong Kong-Macao Joint Laboratory for Environmental Pollution and Control, Guangzhou Institute of Geochemistry, Chinese Academy of Sciences, Guangzhou 510640, China; CAS Center for Excellence in Deep Earth Science, Guangzhou 510640, China;* orcid.org/0000-0002-3637-1642

Hai Guo − *Department of Civil and Environmental Engineering, The Hong Kong Polytechnic University, Kowloon, Hong Kong 999077, China;* orcid.org/0000-0002-7996-7294

Xin Liu − *State Key Laboratory of Organic Geochemistry and Guangdong-Hong Kong-Macao Joint Laboratory for Environmental Pollution and Control, Guangzhou Institute of Geochemistry, Chinese Academy of Sciences, Guangzhou 510640, China*

Guangcai Zhong − *State Key Laboratory of Organic Geochemistry and Guangdong-Hong Kong-Macao Joint Laboratory for Environmental Pollution and Control, Guangzhou Institute of Geochemistry, Chinese Academy of Sciences, Guangzhou 510640, China; CAS Center for Excellence in Deep Earth Science, Guangzhou 510640, China;* orcid.org/0000-0002-5647-5940

Yue Xu − *State Key Laboratory of Environmental Geochemistry, Institute of Geochemistry, Chinese Academy of Sciences, Guiyang 550002, China*

Tian Lin − *College of Marine Ecology and Environment, Shanghai Ocean University, Shanghai 201306, China;* orcid.org/0000-0001-9813-7782

Xiaopu Lyv − *Department of Civil and Environmental Engineering, The Hong Kong Polytechnic University, Kowloon, Hong Kong 999077, China*

Duohong Chen − *State Environmental Protection Key Laboratory of Regional Air Quality Monitoring, Guangdong Environmental Monitoring Center, Guangzhou 510308, China*

Kechang Li − *State Key Laboratory of Organic Geochemistry and Guangdong-Hong Kong-Macao Joint Laboratory for Environmental Pollution and Control, Guangzhou Institute of Geochemistry, Chinese Academy of Sciences, Guangzhou 510640, China*

Jin Shen − *State Environmental Protection Key Laboratory of Regional Air Quality Monitoring, Guangdong Environmental Monitoring Center, Guangzhou 510308, China*

Complete contact information is available at: https://pubs.acs.org/10.1021/acs.est.1c01045

Notes

The authors declare no competing financial interest.

■ ACKNOWLEDGMENTS

This work was supported by the National Key R&D Program of China (2017YFC0212000), Local Innovative Scientific Research Team Project of Guangdong "Pearl River Talents Plan" (2017BT01Z134), Guangdong Foundation for Program of Science and Technology Research (2019B121205006, 2019A1515011254, and 2021A1515012177), and Tuguangchi Award for Excellent Young Scholar GIG and the State Key Laboratory of Organic Geochemistry, GIGCAS (SKLOG2020-9). The authors gratefully thank Xiaofei Geng, Ruiling Zhang,

https://doi.org/10.1021/acs.est.1c01045
Environ. Sci. Technol. 2021, 55, 9740−9749

Zehao Zou, Hongxing Jiang, and Tiangang Tang for their contribution to this work. We also greatly thank all the volunteers helping in the sampling campaign. We appreciate Matthew MacLeod and Fangyuan Zhao from Stockholm University to provide guidance on the application of the BETR Global model. We thank Kevin Jones for kindly offering invaluable advice on revising the manuscript.

REFERENCES

(1) UNEP *The Stockholm Convention on Persistent Organic Pollutants*; United Nations Environmental Programme, 2001.
(2) Wei, D.; Kameya, T.; Urano, K. Environmental management of pesticidal POPs in China: Past, present and future. *Environ. Int.* **2007**, *33*, 894−902.
(3) Zhang, G.; Parker, A.; House, A.; Mai, B. X.; Li, X. D.; Kang, Y. H.; Wang, Z. S. Sedimentary records of DDT and HCH in the Pearl River Delta, South China. *Environ. Sci. Technol.* **2002**, *36*, 3671−3677.
(4) Wang, S.; Steiniche, T.; Romanak, K. A.; Johnson, E.; Quirós, R.; Mutegeki, R.; Wasserman, M. D.; Venier, M. Atmospheric Occurrence of Legacy Pesticides, Current Use Pesticides, and Flame Retardants in and around Protected Areas in Costa Rica and Uganda. *Environ. Sci. Technol.* **2019**, *53*, 6171−6181.
(5) Ya, M.; Wu, Y.; Wu, S.; Li, Y.; Mu, J.; Fang, C.; Yan, J.; Zhao, Y.; Qian, R.; Lin, X.; Wang, X. Impacts of Seasonal Variation on Organochlorine Pesticides in the East China Sea and Northern South China Sea. *Environ. Sci. Technol.* **2019**, *53*, 13088−13097.
(6) Zheng, Q.; Li, J.; Wang, Y.; Lin, T.; Xu, Y.; Zhong, G.; Bing, H.; Luo, C.; Zhang, G. Levels and enantiomeric signatures of organochlorine pesticides in Chinese forest soils: Implications for sources and environmental behavior. *Environ. Pollut.* **2020**, *262*, 114139.
(7) Taiwo, A. M. A review of environmental and health effects of organochlorine pesticide residues in Africa. *Chemosphere* **2019**, *220*, 1126−1140.
(8) Chen, W.; Jing, M.; Bu, J.; Ellis Burnet, J.; Qi, S.; Song, Q.; Ke, Y.; Miao, J.; Liu, M.; Yang, C. Organochlorine pesticides in the surface water and sediments from the Peacock River Drainage Basin in Xinjiang, China: a study of an arid zone in Central Asia. *Environ. Monit. Assess.* **2011**, *177*, 1−21.
(9) Gong, P.; Wang, X.; Pokhrel, B.; Wang, H.; Liu, X.; Liu, X.; Wania, F. Trans-Himalayan Transport of Organochlorine Compounds: Three-Year Observations and Model-Based Flux Estimation. *Environ. Sci. Technol.* **2019**, *53*, 6773−6783.
(10) Ren, J.; Wang, X.; Gong, P.; Wang, C. Characterization of Tibetan Soil As a Source or Sink of Atmospheric Persistent Organic Pollutants: Seasonal Shift and Impact of Global Warming. *Environ. Sci. Technol.* **2019**, *53*, 3589−3598.
(11) Carrizo, D.; Sobek, A.; Salvadó, J. A.; Gustafsson, Ö. Spatial Distributions of DDTs in the Water Masses of the Arctic Ocean. *Environ. Sci. Technol.* **2017**, *51*, 7913−7919.
(12) Bravo, N.; Grimalt, J. O.; Chashchin, M.; Chashchin, V. P.; Odland, J.-O. Drivers of maternal accumulation of organohalogen pollutants in Arctic areas (Chukotka, Russia) and 4,4 '-DDT effects on the newborns. *Environ. Int.* **2019**, *124*, 541−552.
(13) Wang, G.; Lu, Y.; Han, J.; Luo, W.; Shi, Y.; Wang, T.; Sun, Y. Hexachlorobenzene sources, levels and human exposure in the environment of China. *Environ. Int.* **2010**, *36*, 122−130.
(14) Mao, S.; Zhang, G.; Li, J.; Geng, X.; Wang, J.; Zhao, S.; Cheng, Z.; Xu, Y.; Li, Q.; Wang, Y. Occurrence and sources of PCBs, PCNs, and HCB in the atmosphere at a regional background site in east China: Implications for combustion sources. *Environ. Pollut.* **2020**, *262*, 114267.
(15) Lin, T.; Hu, Z.; Zhang, G.; Li, X.; Xu, W.; Tang, J.; Li, J. Levels and Mass Burden of DDTs in Sediments from Fishing Harbors: The Importance of DDT-Containing Antifouling Paint to the Coastal Environment of China. *Environ. Sci. Technol.* **2009**, *43*, 8033−8038.
(16) Schenker, U.; Scheringer, M.; Hungerbühler, K. Investigating the Global Fate of DDT: Model Evaluation and Estimation of Future Trends. *Environ. Sci. Technol.* **2008**, *42*, 1178−1184.
(17) Manaca, M. N.; Grimalt, J. O.; Gari, M.; Sacarlal, J.; Sunyer, J.; Gonzalez, R.; Dobano, C.; Menendez, C.; Alonso, P. L. Assessment of exposure to DDT and metabolites after indoor residual spraying through the analysis of thatch material from rural African dwellings. *Environ. Sci. Pollut. Res.* **2012**, *19*, 756−762.
(18) Manaca, M. N.; Grimalt, J. O.; Sunyer, J.; Mandomando, I.; Gonzalez, R.; Sacarlal, J.; Dobano, C.; Alonso, P. L.; Menendez, C. Concentration of DDT compounds in breast milk from African women (Manhica, Mozambique) at the early stages of domestic indoor spraying with this insecticide. *Chemosphere* **2011**, *85*, 307−314.
(19) Qiu, X. H.; Zhu, T.; Yao, B.; Hu, J. X.; Hu, S. W. Contribution of dicofol to the current DDT pollution in China. *Environ. Sci. Technol.* **2005**, *39*, 4385−4390.
(20) Wang, Q.; Zhao, L.; Fang, X.; Xu, J.; Li, Y.; Shi, Y.; Hu, J. Gridded usage inventories of chlordane in China. *Front. Environ. Sci. Eng.* **2013**, *7*, 10−18.
(21) Bailey, R. E. Global hexachlorobenzene emissions. *Chemosphere* **2001**, *43*, 167−182.
(22) Li, J.; Zhang, G.; Guo, L.; Xu, W.; Li, X.; Lee, C. S. L.; Ding, A.; Wang, T. Organochlorine pesticides in the atmosphere of Guangzhou and Hong Kong: Regional sources and long-range atmospheric transport. *Atmos. Environ.* **2007**, *41*, 3889−3903.
(23) Wang, J.; Guo, L.; Li, J.; Zhang, G.; Lee, C. S. L.; Li, X.; Jones, K. C.; Xiang, Y.; Zhong, L. Passive air sampling of DDT, chlordane and HCB in the Pearl River Delta, South China: Implications to regional sources. *J. Environ. Monit.* **2007**, *9*, 582−588.
(24) Liu, L. The Water-Economy Nexus and Sustainable Transition of the Pearl River Delta, China (1999−2015). *Sustainability* **2018**, *10*, 2595.
(25) National Bureau of Statistics of China. *Statistics Bureau of Guangdong Province Analysis of population development in guangdong of 2019 (in Chinese)*; Guangdong, China, 2019.
(26) Zeren, Y.; Guo, H.; Lyu, X.; Jiang, F.; Wang, Y.; Liu, X.; Zeng, L.; Li, M.; Li, L. An Ozone "Pool" in South China: Investigations on Atmospheric Dynamics and Photochemical Processes Over the Pearl River Estuary. *J. Geophys. Res.: Atmos.* **2019**, *124*, 12340−12355.
(27) Ding, A.; Wang, T.; Fu, C. Transport characteristics and origins of carbon monoxide and ozone in Hong Kong, South China. *J. Geophys. Res.: Atmos.* **2013**, *118*, 9475−9488.
(28) Wang, H.; Lyu, X.; Guo, H.; Wang, Y.; Zou, S.; Ling, Z.; Wang, X.; Jiang, F.; Zeren, Y.; Pan, W.; Huang, X.; Shen, J. Ozone pollution around a coastal region of South China Sea: interaction between marine and continental air. *Atmos. Chem. Phys.* **2018**, *18*, 4277−4295.
(29) Wang, X.; Zong, Z.; Tian, C.; Chen, Y.; Luo, C.; Tang, J.; Li, J.; Zhang, G. Assessing on toxic potency of PM2.5-bound polycyclic aromatic hydrocarbons at a national atmospheric background site in North China. *Sci. Total Environ.* **2018**, *612*, 330−338.
(30) Geng, X.; Mo, Y.; Li, J.; Zhong, G.; Tang, J.; Jiang, H.; Ding, X.; Malik, R. N.; Zhang, G. Source apportionment of water-soluble brown carbon in aerosols over the northern South China Sea: Influence from land outflow, SOA formation and marine emission. *Atmos. Environ.* **2020**, *229*, 117484.
(31) Hsu, Y. K.; Holsen, T. M.; Hopke, P. K. Comparison of hybrid receptor models to locate PCB sources in Chicago. *Atmos. Environ.* **2003**, *37*, 545−562.
(32) Polissar, A. V.; Hopke, P. K.; Harris, J. M. Source Regions for Atmospheric Aerosol Measured at Barrow, Alaska. *Environ. Sci. Technol.* **2001**, *35*, 4214−4226.
(33) Bogdal, C.; Muller, C. E.; Buser, A. M.; Wang, Z. Y.; Scheringer, M.; Gerecke, A. C.; Schmid, P.; Zennegg, M.; MacLeod, M.; Hungerbuhler, K. Emissions of Polychlorinated Biphenyls, Polychlorinated Dibenzo-p-dioxins, and Polychlorinated Dibenzofurans during 2010 and 2011 in Zurich, Switzerland. *Environ. Sci. Technol.* **2014**, *48*, 482−490.
(34) Rodgers, T. F. M.; Truong, J. W.; Jantunen, L. M.; Helm, P. A.; Diamond, M. L. Organophosphate Ester Transport, Fate, and Emissions in Toronto, Canada, Estimated Using an Updated

https://doi.org/10.1021/acs.est.1c01045
Environ. Sci. Technol. 2021, 55, 9740−9749

Multimedia Urban Model. *Environ. Sci. Technol.* **2018**, *52*, 12465−12474.
(35) Zhao, S.; Breivik, K.; Liu, G.; Zheng, M.; Jones, K. C.; Sweetman, A. J. Long-Term Temporal Trends of Polychlorinated Biphenyls and Their Controlling Sources in China. *Environ. Sci. Technol.* **2017**, *51*, 2838−2845.
(36) MacLeod, M.; Riley, W. J.; McKone, T. E. Assessing the Influence of Climate Variability on Atmospheric Concentrations of Polychlorinated Biphenyls Using a Global-Scale Mass Balance Model (BETR-Global). *Environ. Sci. Technol.* **2005**, *39*, 6749−6756.
(37) Wöhrnschimmel, H.; MacLeod, M.; Hungerbuhler, K. Emissions, Fate and Transport of Persistent Organic Pollutants to the Arctic in a Changing Global Climate. *Environ. Sci. Technol.* **2013**, *47*, 2323−2330.
(38) MacLeod, M.; Fraser, A. J.; Mackay, D. Evaluating and expressing the propagation of uncertainty in chemical fate and bioaccumulation models. *Environ. Toxicol. Chem.* **2002**, *21*, 700−709.
(39) Yang, Y.; Li, D.; Mu, D. Levels, seasonal variations and sources of organochlorine pesticides in ambient air of Guangzhou, China. *Atmos. Environ.* **2008**, *42*, 677−687.
(40) Ling, Z. H.; Xu, D. Y.; Zou, S. C.; Lee, S. C.; Ho, K. F. Characterizing the Gas-phase Organochlorine Pesticides in the Atmosphere over the Pearl River Delta Region. *Aerosol Air Qual. Res.* **2011**, *11*, 237−246.
(41) Li, Z.; Zhou, Z.; Gu, T.; Li, S.; Zhang, S.; Liu, D. Organochloride pesticides in the atmosphere of Shenzhen in winter and summer. *China Environm. Sci.* **2011**, *31*, 724−728.
(42) Yu, S. Y.; Liu, W. J.; Xu, Y. S.; Zhao, Y. Z.; Cai, C. Y.; Liu, Y.; Wang, X.; Xiong, G. N.; Tao, S.; Liu, W. X. Organochlorine pesticides in ambient air from the littoral cities of northern China: Spatial distribution, seasonal variation, source apportionment and cancer risk assessment. *Sci. Total Environ.* **2019**, *652*, 163−176.
(43) Syed, J. H.; Malik, R. N.; Liu, D.; Xu, Y.; Wang, Y.; Li, J.; Zhang, G.; Jones, K. C. Organochlorine pesticides in air and soil and estimated air−soil exchange in Punjab, Pakistan. *Sci. Total Environ.* **2013**, *444*, 491−497.
(44) Wang, W. T.; Wang, Y. H.; Zhang, R. J.; Wang, S. P.; Wei, C. S.; Chaemfa, C.; Li, J.; Zhang, G.; Yu, K. F. Seasonal characteristics and current sources of OCPs and PCBs and enantiomeric signatures of chiral OCPs in the atmosphere of Vietnam. *Sci. Total Environ.* **2016**, *542*, 777−786.
(45) Yu, H.-Y.; Bao, L.-J.; Liang, Y.; Zeng, E. Y. Field Validation of Anaerobic Degradation Pathways for Dichlorodiphenyltrichloroethane (DDT) and 13 Metabolites in Marine Sediment Cores from China. *Environ. Sci. Technol.* **2011**, *45*, 5245−5252.
(46) Zhang, C.; Liu, L.; Ma, Y.; Li, F. Using Isomeric and Metabolic Ratios of DDT To Identify the Sources and Fate of DDT in Chinese Agricultural Topsoil. *Environ. Sci. Technol.* **2018**, *52*, 1990−1996.
(47) Qiu, X.; Zhu, T. Using the o,p′-DDT/p,p′-DDT ratio to identify DDT sources in China. *Chemosphere* **2010**, *81*, 1033−1038.
(48) Wu, C. C.; Sao, L. J.; Tao, S.; Zeng, E. Y. Significance of antifouling paint flakes to the distribution of dichlorodiphenyltrichloroethanes (DDTs) in estuarine sediment. *Environ. Pollut.* **2016**, *210*, 253−260.
(49) Peng, S.; Kong, D.; Li, L.; Zou, C.; Chen, F.; Li, M.; Cao, T.; Yu, C.; Song, J.; Jia, W.; Peng, P. a. Distribution and sources of DDT and its metabolites in porewater and sediment from a typical tropical bay in the South China Sea. *Environ. Pollut.* **2020**, *267*, 115492.
(50) Liu, X.; Zhang, G.; Li, J.; Yu, L. L.; Xu, Y.; Li, X. D.; Kobara, Y.; Jones, K. C. Seasonal Patterns and Current Sources of DDTs, Chlordanes, Hexachlorobenzene, and Endosulfan in the Atmosphere of 37 Chinese Cities. *Environ. Sci. Technol.* **2009**, *43*, 1316−1321.
(51) Yuan, M.; Xu, Y.; Li, S.; Zhang, X.; Pan, Z. Safety evaluation and analysis of small-scale reservoir in Guangdong. *Dam and Safety* **2019**, *4*, 20−23.
(52) Li, J.; Zhang, G.; Qi, S.; Li, X.; Peng, X. Concentrations, enantiomeric compositions, and sources of HCH, DDT and chlordane in soils from the Pearl River Delta, South China. *Sci. Total Environ.* **2006**, *372*, 215−224.
(53) Jantunen, L. M. M.; Bidleman, T. F.; Harner, T.; Parkhurst, W. J. Toxaphene, Chlordane, and Other Organochlorine Pesticides in Alabama Air. *Environ. Sci. Technol.* **2000**, *34*, 5097−5105.
(54) Hung, H.; Halsall, C. J.; Blanchard, P.; Li, H. H.; Fellin, P.; Stern, G.; Rosenberg, B. Temporal Trends of Organochlorine Pesticides in the Canadian Arctic Atmosphere. *Environ. Sci. Technol.* **2002**, *36*, 862−868.
(55) Bioassay of heptachlor for possible carcinogenicity. *Natl. Cancer Inst. Carcinog Tech. Rep. Ser.* **1977**, *9*, 1−109.
(56) Zhan, L.; Lin, T.; Wang, Z.; Cheng, Z.; Zhang, G.; Lyu, X.; Cheng, H. Occurrence and air-soil exchange of organochlorine pesticides and polychlorinated biphenyls at a CAWNET background site in central China: Implications for influencing factors and fate. *Chemosphere* **2017**, *186*, 475−487.
(57) Li, J.; Lin, T.; Qi, S.; Zhang, G.; Liu, X.; Li, K. Evidence of local emission of organochlorine pesticides in the Tibetan plateau. *Atmos. Environ.* **2008**, *42*, 7397−7404.
(58) Navarro, I.; de la Torre, A.; Sanz, P.; Arjol, M. A.; Fernández, J.; Martínez, M. A. Organochlorine pesticides air monitoring near a historical lindane production site in Spain. *Sci. Total Environ.* **2019**, *670*, 1001−1007.
(59) Stemmler, I.; Lammel, G. Cycling of DDT in the global environment 1950−2002: World ocean returns the pollutant. *Geophys. Res. Lett.* **2009**, *36*, L24602.
(60) Wu, Z.; Lin, T.; Hu, L.; Guo, T.; Guo, Z. Atmospheric legacy organochlorine pesticides and their recent exchange dynamics in the Northwest Pacific Ocean. *Sci. Total Environ.* **2020**, 138408.
(61) Yu, H.-Y.; Shen, R.-L.; Liang, Y.; Cheng, H.; Zeng, E. Y. Inputs of antifouling paint-derived dichlorodiphenyltrichloroethanes (DDTs) to a typical mariculture zone (South China): Potential impact on aquafarming environment. *Environ. Pollut.* **2011**, *159*, 3700−3705.
(62) Lo, J. C. F.; Lau, A. K. H.; Fung, J. C. H.; Chen, F. Investigation of enhanced cross-city transport and trapping of air pollutants by coastal and urban land-sea breeze circulations. *J. Geophys. Res.* **2006**, *111*, 115492.
(63) Dumanoglu, Y.; Gaga, E. O.; Gungormus, E.; Sofuoglu, S. C.; Odabasi, M. Spatial and seasonal variations, sources, air-soil exchange, and carcinogenic risk assessment for PAHs and PCBs in air and soil of Kutahya, Turkey, the province of thermal power plants. *Sci. Total Environ.* **2017**, *580*, 920−935.
(64) Li, Y.-F.; Cai, D. J.; Singh, A. Historical DDT use trend in China and usage data gridding with 1/4° by 1/6° longitude/latitude resolution. *Adv. Environ. Res.* **1999**, *2*, 497−506.
(65) Zhao, L. *Usage Inventories for Selected Persistent Organic Pollutants in China*; Peking University: Beijing, 2005.

https://doi.org/10.1021/acs.est.1c01045
Environ. Sci. Technol. 2021, 55, 9740−9749